STUDIES OF AN EXPANDED PLASMA FRONT DUOPLASMATRON ION SOURCE*

J. A. Fasolo
Midwestern Universities Research Association
Stoughton, Wisconsin

Summary

A new and more flexible ion source assembly has been built for continued study of a duoplasmatron with an expanded plasma front and a cylindrical Pierce-electrode extraction geometry. Studies of conditions necessary for the formation of an expanded plane plasma boundary are discussed, and progress toward the achievement of an aberration-free parallel beam of several hundred mA of protons is reviewed. Recent studies suggest that a duoplasmatron with an expanded plasma front and a diverging Pierce-electrode extraction geometry would produce significantly higher aberration-free beam currents than can be obtained with the present cylindrical geometry. The information necessary for the design of lens optics for matching such a source, or any source which produces a diverging aberration-free beam, to an accelerator or plasma containment device is provided in a convenient and comprehensive form by beam characteristic curves which give beam radius and divergence as functions of perveance at some convenient measuring plane close to the extractor for several fixed values of arc current. Data provided by a constant perveance experiment establish practical limits on obtainable beam current at the chosen design points on the characteristic curves.

Introduction

The source used in our earlier studies of a duoplasmatron[1] with an expanded plasma front[2] and a cylindrical Pierce-electrode extraction geometry,[3] Source I, is now installed on the MURA high gradient column[4] at the ANL high voltage test facility, where it is being used by C. D. Curtis in his studies of the column. Source studies at MURA are continuing with a new source assembly.

Development of Source I has been reviewed elsewhere.[5] One modification of this source, Geometry 35, has been studied more thoroughly than any other geometry, and its performance will be considered here in further detail.

*Work performed under the auspices of the U. S. Atomic Energy Commission.

Geometry 35

A complete assembly drawing for Geometry 35 does not exist. It differs from Geometry 30, shown in Fig. 1, only in the geometry and location of the nonmagnetic aperture plate. The single aperture of Geometry 30 has been replaced with three 32-mil diameter apertures with centers equally spaced on a 52-mil diameter circle, and the 40-mil thick aperture plate is 1/16-in. closer to the intermediate electrode.

A method of systematically determining and displaying the characteristics of a given source geometry has been applied to Geometry 35. For given values of arc current, extraction voltage and source pressure, beam current, radius and divergence are measured at the location of a slit plate 2.13 in. from the extraction grid as the source magnet is varied over all or most of its range. Beam radius and divergence are then plotted as functions of perveance. If several runs are made with different arc currents, families of characteristic curves are obtained (Fig. 2).

For each arc current, there is a transition region in which r_{max} and $\tan \theta_{max}$ are multiple valued functions of perveance. Below the transition, a distorted beam is obtained; above, the beam is distortion free. There is a significant increase in beam loading on the extraction voltage in this region and the transition apparently occurs when the beam diameter becomes as large or larger than the aperture in the extractor.

The difference in quality on the two sides of the transition is evidently due to the edge effect that results from the fact that the plasma and the Pierce electrode are not at the same potential and do not form a continuous boundary at anode potential. Above the transition, beam edge particles are intercepted by the extractor, and the secondary slit images to which they give rise are eliminated.

In cases where an aberration-free diverging beam would be acceptable, beam loss on the extractor could be reduced, without introducing aberrations, by using a diverging Pierce-electrode extraction geometry.[5]

It may be noted that the characteristic curves shift to higher perveance as the arc current is increased. It is shown in reference 5 that for a given plasma boundary perveance is related to effective mass number by an equation of the form $P_s M^{1/2}$ = const., while the particle trajectories are independent of M. The shift of the curves to higher perveance can thus be attributed to a corresponding decrease in $M^{1/2}$ with increasing arc current.

Beam characteristic curves provide all of the information necessary for the design of lens optics for matching a source to an accelerating column or plasma containment device. The data obtained in a constant perveance experiment at the chosen design points on the characteristic curves provide the additional information required to vary source, lens and column parameters so that particle trajectories remain constant over a range of beam currents. They also establish practical limits on obtainable beam current since eventually a point is reached where maximum permissible source, lens or column gradients are exceeded or the source cannot be adjusted to give a plasma of the required density.

The results of a constant perveance experiment are shown in Fig. 3, where the bright spot at the center of each beam image results from the fact that the aluminum coating on the viewing screen was semitransparent and transmitted light from the arc. The beam is pulsed (six 200-μs pulses per second) and photographic exposure was varied in approximate accordance with a formula given by Spangenberg[6] for exposure time in the photography of recurrent traces, $t = K F^2 (M + 1)^2 w^{-1}$, where K is a constant, F is lens stop, M is image magnification and w is beam power density.

Since r_{max} is constant, the constancy of the width of the on-axis image implies that the area of the emittance diagram is a constant. It follows that the normalized emittance varies as the one-third power of the beam current when the perveance is kept constant. It also follows that the normalized emittance varies as the one-half power of magnetic field strength, from the linear variation in magnet current with voltage.

In reference 5 it was incorrectly stated that the particular slit plate used in most of our studies of Source I had 15-mil wide slits when, in fact, the slits were only 10-mils wide. Using the correct value, we find that the area of the emittance diagram for the constant perveance experiment is 8.5 cm-mrad, rather than the negative value that resulted from a misunderstanding, on the part of this writer, of the precision, or lack thereof, with which the plates were manufactured.[7]

If there is a variation in perveance during a pulse, $Z_s = r_{max}/\tan \theta_{max}$ will also vary during the pulse, and there will be a corresponding variation in the width of the slit images. There is a difference (measured on a photograph) between the width of the nth off-axis image and that of the on-axis image which is given by $\Delta W_m(n) = nS \Delta r \Delta Z_s/(R Z_{s1} Z_{s2})$ where S is target-screen separation, Δr is slit separation and R is the ratio of the actual size to the size measured on a photograph.

In some cases $\Delta W_m(n)$ is measurable; in others it is not, because the variation of Z_s with perveance is greatest at low perveance, where little difficulty is encountered in obtaining a flat-topped beam pulse, and least at high perveance, where it is sometimes difficult to obtain a flat-topped pulse. The presence of high frequency oscillations on a flat-topped pulse can, however, result in a measurable broadening of the lines at low perveance. For Geometry 35, these oscillations are most severe for magnet currents less than 0.4 A.

The linear variation in magnet current, or magnetic field, with extraction voltage is an apparent violation of a well known scaling law, $V B^{-2} L^{-2}$ = const., which relates voltage, magnetic field and linear dimension when applied to the motion of charged particles in combined electric and magnetic fields. This suggests that the diverging magnetic field in the extraction region is too weak to have a measurable effect on accelerated ion trajectories. On the other hand, results of a magnetic field-shaping experiment indicate that even though the field is too weak to affect accelerated ion trajectories its shape has an easily measurable effect.[5] Evidently, the effect is on the shape of the plasma boundary and consequently on the initial directions of acceleration of the ions rather than on their subsequent motions in combined fields.

Additional conclusions have been drawn from the results of this constant perveance experiment by C. D. Curtis.[8]

From the results obtained with Geometry 35, it is evident that three conditions are necessary for the formation of a plane plasma boundary and an aberration-free parallel beam. The

first, of course, is a uniform radial plasma density distribution. The second is the elimination of the edge effect that results from the fact that the plasma and the Pierce electrode do not form a continuous boundary at anode potential or, if it cannot be eliminated, the interception of beam edge particles by using an extractor aperture somewhat smaller than the ideal beam diameter. The third requirement is a magnetic field that, if finite, is parallel to the axis in the neighborhood of the plasma boundary and too weak to affect accelerated ion trajectories outside of this region.

Shaped Field Source Assembly

Although the results obtained with a coil mounted in the extraction electrode showed that the high divergence of the beam produced on the high perveance side of the transition region could be reduced with a coil at this location, it was decided not to pursue this approach any further, because the space required for a coil would interpose a drift space between the extraction region and the accelerator and prevent direct injection into the column or an electrostatic focusing section.

The source built to replace Source I was tested briefly in a configuration similar to Geometry 35 to insure that results obtained with that geometry could be duplicated with the new source. On the basis of information and insights obtained in a magnet modeling program the new source was then modified by the addition of two field-shaping magnets. The modified assembly is shown in Fig. 4, where mild steel portions of the magnetic circuits are shown cross hatched. The source is forced-air cooled by means not shown in the drawing, and the source magnet was subdivided to increase cooling surface area.

The manner in which the first shaping magnet (M-2) modifies the axial distribution produced by the source magnet (M-1) is shown in Fig. 5. An aiding field has a detrimental effect on the distribution while an opposing field improves it. Similar data for M-3, in Fig. 6, show that a more uniform field can also be obtained in the extraction region with an aiding M-3 field, but the magnitude of the resultant field is greater than that for the opposing M-2 case of Fig. 5.

A study comparable to that of Geometry 35 has not yet been made with this assembly, but preliminary results are encouraging–and puzzling. The beam images shown in Fig. 7 were taken within five minutes of each other during a preliminary run in which both of the field shaping magnets were turned off. The image on the left, for which no data were taken, is unlike any that was ever obtained with Source I, or with the Source I-type geometry tested before the addition of the field shaping magnets. The image on the right is for a 90 mA (average), 17 keV beam with a normalized emittance of 0.013 cm-mrad, a radius of 0.614 in. and a divergence of 0.182 rad. In Fig. 2, at a perveance of 1.29 $mA/(kV)^{3/2}$, we find $r_{max} = 0.89$ in. and $\tan \theta_{max} = 0.29$ rad for the best values obtained with Geometry 35.

During the course of efforts to find and eliminate the cause of the type of image shown on the left in Fig. 7, a number of isolated instances of beam of very good quality have been encountered, in addition to the example shown on the right in Fig. 7. Because they are isolated instances, rather than parts of a systematic study, they contribute nothing to a better understanding of this geometry and will not be considered here.

The cause of the distorted images has not yet been found, but it has been observed that they are not obtained at low beam power density. It has also been found that the aluminum coating on the glass screen is damaged or destroyed much more rapidly and thoroughly than ever before, perhaps because of contaminants existing in the source or introduced in the coating process.

Acknowledgments

The author has benefited from numerous useful and enlightening discussions with C. D. Curtis. The design of the source and the test facility owe much to the contributions of G. M. Lee. Power supplies other than the high voltage supply were designed and developed by R. L. Bennett who has also done much to improve the electronic circuitry. The assistance of J. Mayes in the experimental work is greatly appreciated, as are the efforts of L. Siverling and others too numerous to mention.

References

1. M. von Ardenne, Tabellen der Elektronenphysik, Ionenphysik und Übermikroscopie I, 544-549, V. E. B. Deutscher Verlag der Wissenschaften (Berlin, 1956).

2. J. A. Fasolo, Analysis of von Ardenne's Duoplasmatron and Comparison with the Livermore High Current Ion Injector, LRL Engineering Note CVL-1, Oct. 1, 1957 (unpublished).

3. J. R. Pierce, Theory and Design of Electron Beams, 2 d Ed., D. Van Nostrand Company, Inc., Princeton, N. J. (1954).

4. C. D. Curtis et al., Tests of the MURA High Gradient Column, The 1966 Linear Accelerator Conference held at Los Alamos Scientific Laboratory, Los Alamos, New Mexico, October 3-7, 1966.

5. J. A. Fasolo et al., Duoplasmatron Source Performance at MURA, The 1966 Linear Accelerator Conference, held at Los Alamos Scientific Laboratory, Los Alamos, New Mexico, October 3-7, 1966.

6. K. R. Spangenberg, Vacuum Tubes, McGraw-Hill, New York (1940), p. 472.

7. J. A. Fasolo, Corrected Results of a Constant Perveance Experiment, MURA TN-634 (unpublished).

8. C. D. Curtis, Expectations and Possible Interpretation of Ion Source Behavior, The 1966 Linear Accelerator Conference, held at Los Alamos Scientific Laboratory, Los Alamos, New Mexico, October 3-7, 1966.

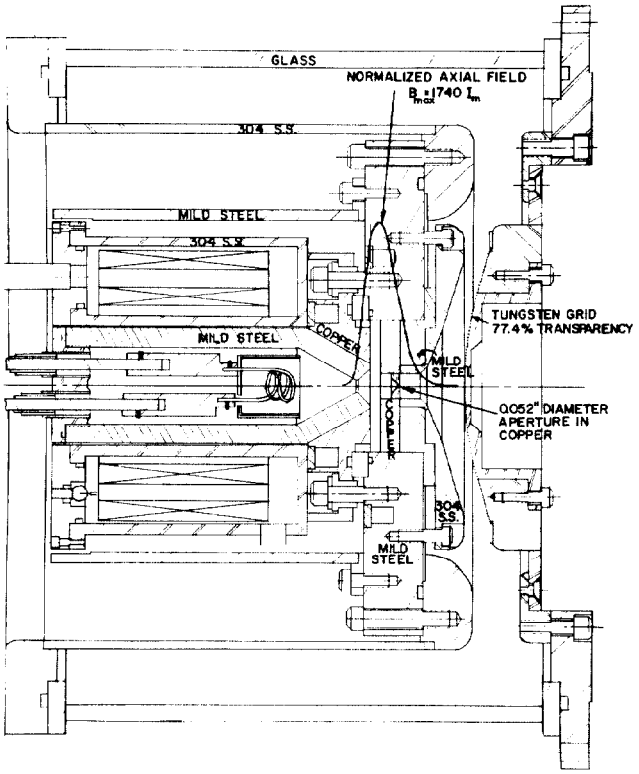

Fig. 1. Geometry 30, Source I.

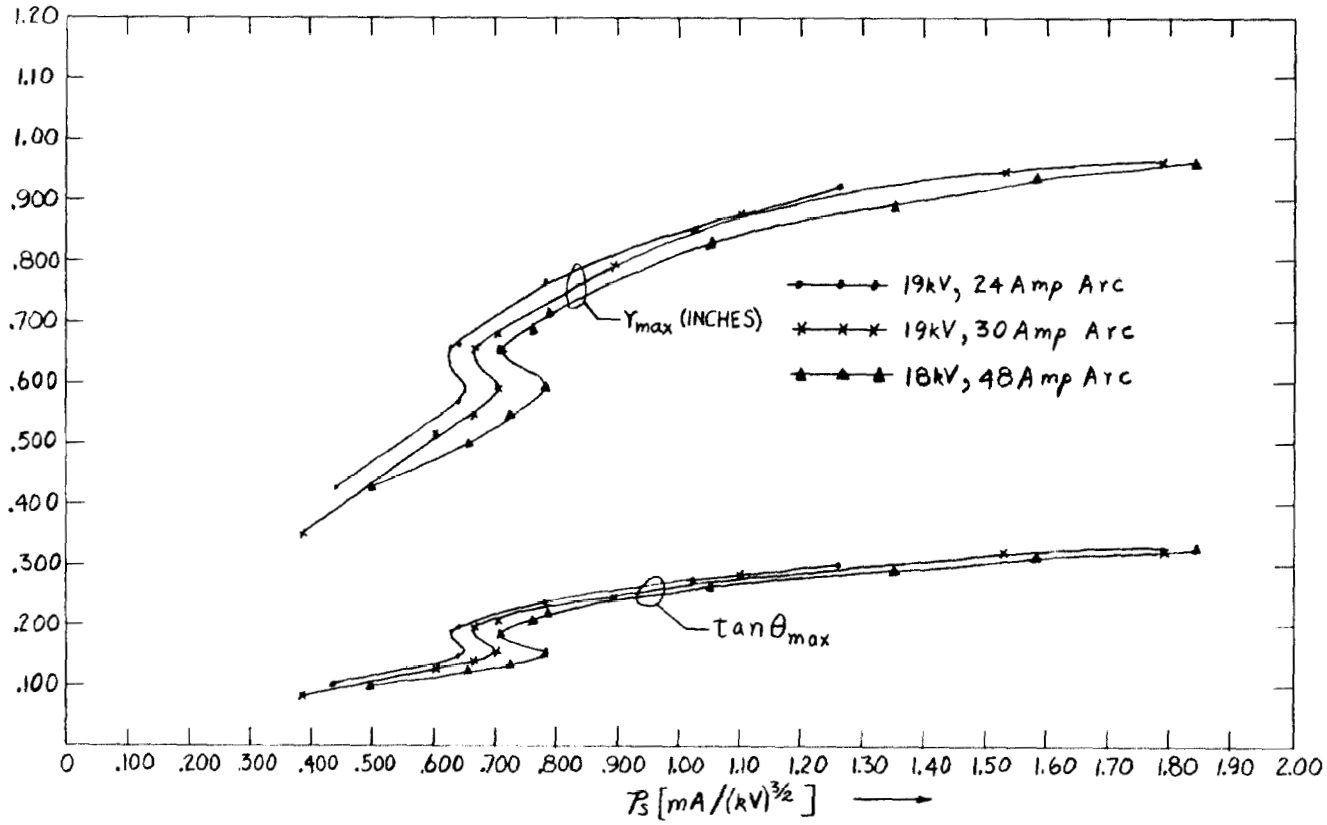

Fig. 2. Characteristic Curves for Geometry 35.

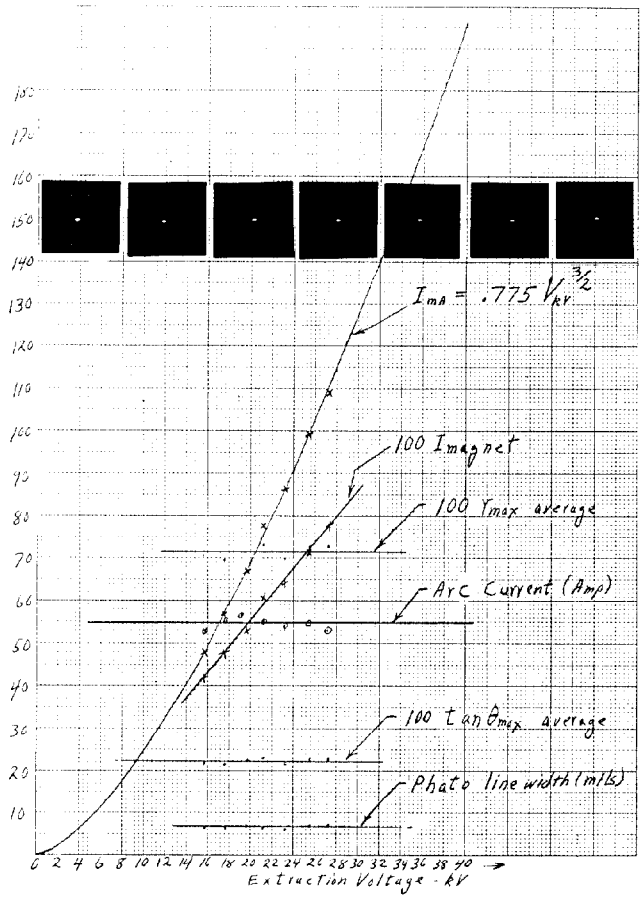

Fig. 3. Results of a Constant Perveance Experiment.

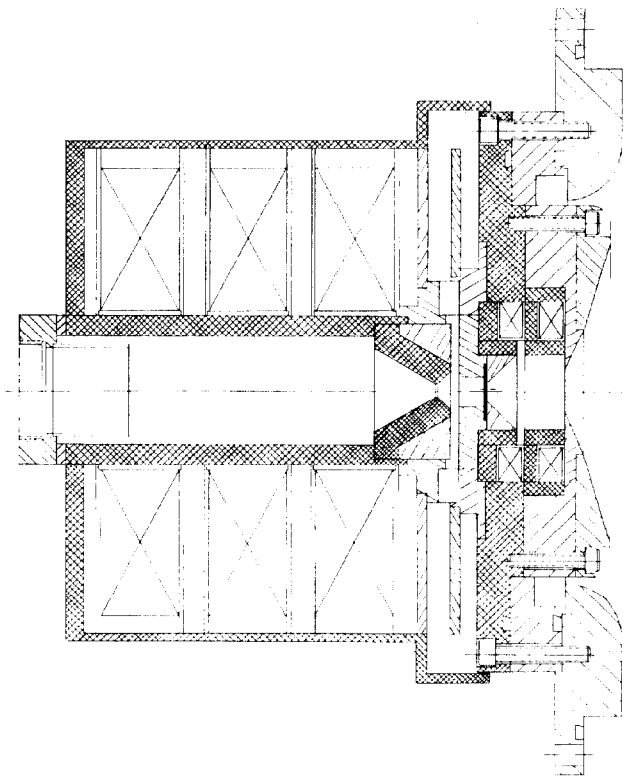

Fig. 4. Shaped Field Source Assembly.

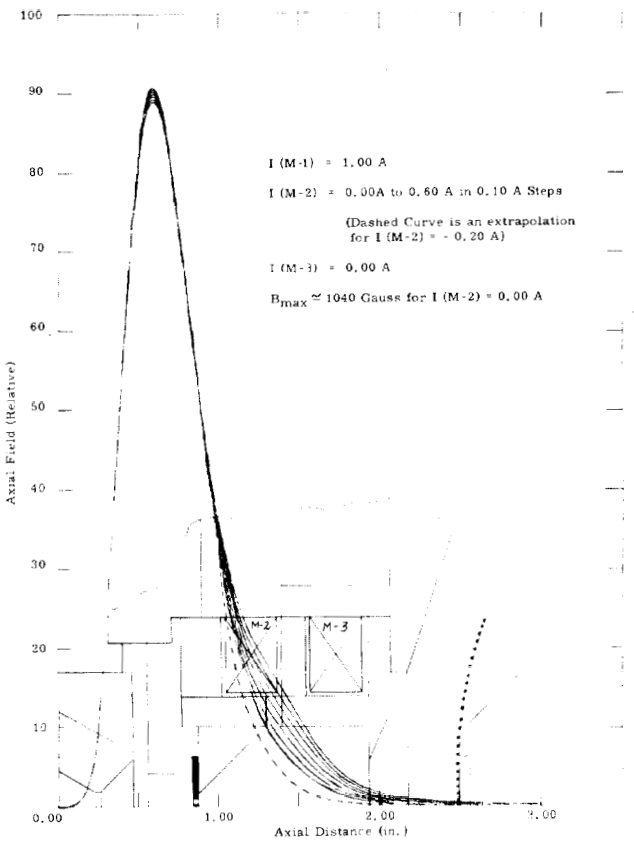

Fig. 5. Affect of M-2 on Axial Field Distribution.

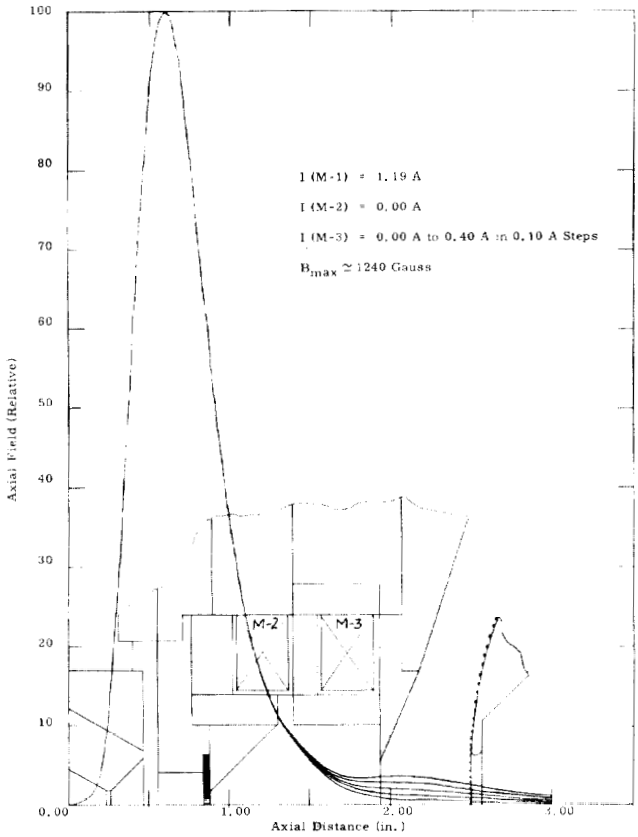

Fig. 6. Affect of M-3 on Axial Field Distribution.

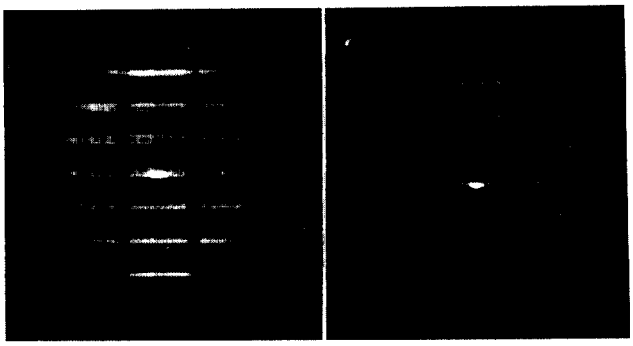

Fig. 7. Examples of Anomalous and Normal Beam Images. The Aperture Plate is at the 81% Axial Field Point (Fig. 6).